Direct and Split Operator Approaches with ELLAM for Reactive Transport Equations

Anis Younes and Marwan Fahs
Institut de Mécanique des Fluides et des Solides, UMR CNRS-ULP 7507, 2, rue Boussingault, 67000 Strasbourg, France

DOI 10.1002/aic.11234
Published online June 28, 2007 in Wiley InterScience (www.interscience.wiley.com).

Numerical models for solving reactive solute transport in groundwater are often based on standard Eulerian methods, such as finite elements (FE). In this work, we combine the moving mesh Eulerian Lagrangian Localized Adjoint Method (ELLAM) with the direct substitution approach (DSA) and the sequential non-iterative approach (SNIA) to accurately solve advection dominated problems including chemical reactions. Performances of ELLAM are evaluated in comparing SNIA_ELLAM and DSA_ELLAM to SNIA_FE and DSA_FE for (1) kinetic reactions with first-order decay, Monod biodegradation, and interphase mass transfer problems and (2) equilibrium reactions with linear and nonlinear sorption problems. DSA_ELLAM (respectively SNIA_ELLAM) is shown to be more efficient and accurate than DSA_FE (respectively SNIA_FE). For the test cases with kinetics, SNIA_ELLAM is highly accurate and efficient. However, for equilibrium reactions, it induces numerical diffusion and DSA_ELLAM reveals the more efficient and accurate method. © 2007 American Institute of Chemical Engineers *AIChE J,* 53: 2161–2169, 2007
Keywords: finite elements, moving mesh, Eulerian Lagrangian localized adjoint method, reactive transport, operator splitting

Introduction

Contaminant transport problems such as transfer with biological, chemical, or radioactive processes in porous media are often described with mathematical models including a set of coupled nonlinear advective-diffusive-reactive transport equations. Because of the nonlinearity, accurate and efficient simulators remain a challenge, even in one dimension, particularly for problems with sharp concentration fronts. The multicomponent transport equations can be written as:

$$\frac{\partial C_i}{\partial t} = -U\frac{\partial C_i}{\partial x} + \frac{\partial}{\partial x}\left(D_i\frac{\partial C_i}{\partial x}\right) + f_i(C_1,\ldots,C_{Nc},t), \quad i=1,\ldots,Nc \tag{1}$$

Variations in concentration of each mobile species C_i are caused by advection, with velocity U, dispersion, with dispersion coefficient D_i and reaction intensity f_i. The reaction terms f_i can be nonlinear function of all the Nc species.

The nonlinear system (1) can be solved by successive convergence iterations with a global direct substitution approach (DSA) and using Picard or Newton-Raphson methods. In this case, chemical and transport equations are solved simultaneously. DSA is known to be much more difficult to implement than operator splitting (OS) schemes and can become very demanding in terms of computing time and memory capacity.[1] However, DSA avoids the splitting operator errors and is therefore considered to be more accurate than OS.[2–6]

OS approach usually splits the nonlinear system of advection dispersion reaction equations (1) into a system of linear partial differential equations just including the advection and dispersion terms to find a trial solution $C_i^{n+1,*}$.

$$C_i^{n+1,*} = C_i^n + \int_t^{t+\Delta t}\left(-U\frac{\partial C_i}{\partial x} + \frac{\partial}{\partial x}\left(D_i\frac{\partial C_i}{\partial x}\right)\right)dt, \quad i=1,\ldots,Nc \tag{2}$$

Correspondence concerning this article should be addressed to A. Younes at younes@imfs.u-strasbg.fr.

Then, this trial solution is used as initial condition for the resolution of a second system formed by the nonlinear ordinary differential reaction equations:

$$C_i^{n+1} = C_i^{n+1,*} + \int_t^{t+\Delta t} f_i(C_1,\ldots,C_{Nc},t)dt, \quad i=1,\ldots,Nc \qquad (3)$$

Since the reference work by Yeh and Tripathi,[7] the OS approach is widely used to simulate reactive transport problems. This approach has many advantages: (i) it can easily be implemented, (ii) OS leads to a smaller system than DSA, which may be solved with parallel implementations,[8] (iii) transport and chemistry can be solved using different numerical techniques that are specifically suited to achieve high accuracy for each system of equations,[2,9] and (iv) chemistry can be solved using subtime steps which can be much smaller than the time step for the transport since the characteristic times of transport are often much larger than that of reaction equations.[3]

On the other hand, it is well known that the advection dispersion reaction equation (ADRE) itself is difficult to solve because of its hyperbolic nature due to the advection term. This term is usually modeled with standard Eulerian methods such as finite elements (FE) or finite volumes, which may cause severe numerical oscillations and instability, especially in the presence of sharp fronts.[4]

The Eulerian-Lagrangian localized adjoint method (ELLAM) is an improved characteristic method. ELLAM has the same performance as characteristic methods, guaranties mass conservation, and treats general boundary conditions naturally in its formulation. A highly accurate scheme avoiding spatial interpolation or equivalently numerical integration, which is a major problem in conventional ELLAM formulations, was developed in combining a finite volume ELLAM with a moving grid procedure.[10] The scheme avoids nonphysical oscillations and numerical diffusion whatever the time step used.

In this work, we combine the moving mesh ELLAM with sequential non-iterative approach (SNIA) and DSA to solve accurately advection-dominated reactive transport problems. Five test cases are set up for comparing SNIA_ELLAM and DSA_ELLAM to SNIA_FE and DSA_FE. The test cases are meant to cover a wide spectrum of chemical difficulties and concern (1) kinetic reactions with first-order decay, Monod biodegradation and interphase mass transfer problems and (2) equilibrium reactions with linear and nonlinear sorption problems.

The Finite Volume Moving Mesh ELLAM

Consider the following one-dimensional ADRE with first-order decay:

$$\frac{\partial(RC)}{\partial t} + \frac{\partial(qC)}{\partial x} + KC - \frac{\partial}{\partial x}\left(D\frac{\partial C}{\partial x}\right) = 0 \qquad (4)$$

where q is Darcy's velocity (LT^{-1}), K a first-order reaction coefficient (T^{-1}) and R a retardation coefficient. The equation is defined in the spatial-time domain $\Omega_{xt} = [0,l] \times [0,T]$. For the sake of simplicity, we consider only the following initial and boundary conditions:

$$C(x,0) = C_0(x),\ C(0,t) = g(t), \quad \text{and} \quad \left(-D\frac{\partial C}{\partial x}\right)_{x=l} = 0$$

The spatial domain $\Omega = [0,l]$ is partitioned by *nm* intervals or finite volumes $\Omega_i^0 = [x_{i-1/2}^0, x_{i+1/2}^0]$ of distance Δx_i^0, where x_i^0 is the center of the interval. Evolution in time is divided into discrete but not necessarily equal time steps $\Delta t^{n+1} = t^{n+1} - t^n$.

With Eulerian methods, Eq. 4 is solved over a fixed spatial frame. Classical Eulerian methods are FE and finite differences. For an advection-dominated transport, these methods often generate numerical solutions with artificial diffusion or nonphysical oscillations. Upwind methods give first order accurate stable schemes (without oscillations) but with much artificial diffusion smearing the concentration front.

Another class of methods are characteristic methods. They use a Lagrangian treatment of the advective part by tracking particles along the characteristics and Eulerian treatment on a fixed grid of the dispersive part. ELLAM is an improved characteristic method introduced first by Celia et al.[11] ELLAM uses space-time test functions, guaranties mass conservation and treats "naturally" the general boundary conditions in its formulation.

Different ELLAM schemes based on different (forward or backward) techniques for the tracking along the characteristics are investigated.[12] The ELLAM was also used for reactive transport.[13–16] The ongoing literature often reports on several criticisms to ELLAM (in particular when coupled with chemical reactions) since they may show numerical dispersion or oscillations. Indeed, conventional ELLAM formulations use a fixed grid, defining the solution and the test functions associated with the fixed grid at each time step. Because the location of the foot of the characteristic does not coincide with a grid point, interpolation is necessary at each time step. When many interpolations are necessary (many time steps), numerical diffusion becomes significant. With higher order interpolation, negative weights will be necessary to avoid numerical diffusion, generating potential spurious oscillations.[17]

A highly accurate scheme avoiding spatial interpolation was developed by combining a finite volume ELLAM with a moving grid procedure.[10] The new scheme removes nonphysical oscillations and numerical diffusion whatever the time step used.

The moving mesh ELLAM

The weak formulation of Eq. 4, using space-time test function $\omega = \omega(x,t)$ is written as:

$$\int_0^T \int_\Omega \left[\frac{\partial(RC)}{\partial t}\omega + \frac{\partial(qC)}{\partial x}\omega + KC\omega - \frac{\partial}{\partial x}\left(D\frac{\partial C}{\partial x}\right)\omega\right]dxdt = 0 \qquad (5)$$

The ELLAM selects the test function $\omega_i(x,t)$ with the following property:

$$\frac{\partial \omega_i}{\partial t} + \frac{q}{R}\frac{\partial \omega_i}{\partial x} - \frac{K}{R}\omega_i = 0 \qquad (6)$$

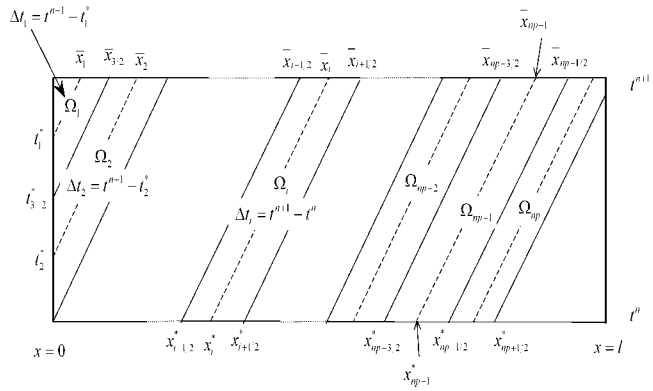

Figure 1. Example of subdomains between and in the case of linear transport with constant coefficients.

which, of course screens the advection part and the chemical decay of the general Eq. 5. Thus, with this choice for ω, the ADRE (5) becomes:

$$\int_{\bar{x}_{i-1/2}}^{\bar{x}_{i+1/2}} R^{n+1}\omega_i^{n+1}C^{n+1} + \int_0^{\Delta t}\int_{\Omega}\frac{\partial}{\partial x}\left[\left(qC - D\frac{\partial C}{\partial x}\right)\omega_i\right]dxdt + \Delta t_i \int_{\Omega} D\frac{\partial C}{\partial x}\frac{\partial \omega_i}{\partial x}dxdt = \int_{x_{i-1/2}^*}^{x_{i+1/2}^*} R^n\omega_i^n C^n \qquad (7)$$

The first term corresponds to the mass at the new time level, the second one to the boundary conditions, the third one to the exchange by dispersion and the right term corresponds to the mass at the old time level. Note that the time step size $\Delta t_i = t^{n+1} - t_i^*$ in the dispersion integral is defined for each element. Indeed, the time step is automatically reduced for elements which backtrack to the inflow boundary during the time period Δt. For example, in Figure 1, we have $\Delta t_1 = t^{n+1} - t_1^* < \Delta t_2 = t^{n+1} - t_2^* < \Delta t_{i>2} = \Delta t = t^{n+1} - t^n$.

The moving mesh

The initial spatial discretization contains nm intervals Ω_i^0 centered at x_i^0. We consider that subdomains Ω_i are dependent on the time step number and we set $\Omega_i = \Omega_i(t^{n+1})$. To define $\Omega_i(t^{n+1})$ for each time step, we compute $\bar{x}_{i\pm1/2}(t^{n+1})$ which is the location at $t = t^{n+1}$ obtained when forward tracking from $x^*_{i\pm1/2}(t^{n+1})$ at $t = t^n$ (with $x^*_{i\pm1/2}(t^1) = x^0_{i\pm1/2}$).

To avoid interpolation, the point at the foot of the characteristic between t^n and t^{n+1} corresponds to the point at the head of the characteristic between t^{n-1} and t^n:

$$x^*_{i\pm1/2}(t^{n+1}) = \bar{x}_{i\pm1/2}(t^n) \qquad (8)$$

The inflow boundary is discretized as shown in Figure 1 in order to account for the mass entering into the domain from the inflow boundary between t^n and t^{n+1}. New P nodes are added at the inflow boundary ($x_j^* = 0,\ j = 1..P$) with different initial times ($t^n < t_j^* < t^{n+1}$) that are forward tracked to $\bar{x}_j > 0$ at $t = t^{n+1}$. Thus, the number of subdomains Ω_i does not remain constant over time and has to be adapted from one time step to the other. Hence, Eq. 8 is replaced with:

$$x^*_{i+p(t^{n+1})\pm1/2}(t^{n+1}) = \bar{x}_{i\pm1/2}(t^n) \qquad (9)$$

During Δt^{n+1}, we assume that a number $r(t^{n+1})$ of subdomains leave the domain from the outflow boundary. Hence, the number of subdomains is given by

$$\forall n \geq 0,\ np(t^{n+1}) = np(t^n) + p(t^{n+1}) - r(t^{n+1}) \quad \text{with } np(t^0) = nm \qquad (10)$$

The time step Δt_i for the dispersion integral in Eq. 7 for each subdomain Ω_i is $\Delta t_i = t^{n+1} - t_i^*$.

The final system

We choose the test function ω_i in the Eq. 5 to be exponential along the characteristic:

$$\omega_i(x,t) = \exp\left[\int_{t^n}^{t}\frac{K}{R}d\theta\right] \qquad (11)$$

The different integrals in Eq. 5 are then evaluated on the moving mesh using standard approximations.[10] The method leads to a tridiagonal system, which can be easily solved to obtain the concentration on the moving mesh.

The Reactive Operator

With OS, chemistry equations can be solved using a numerical technique specifically suited to achieve high accuracy.[2]

When chemical reactions are fast enough so that equilibrium can be assumed, the reaction term f_i corresponds to the temporal variation of S_i, the fixed concentration of the species C_i ($f_i = -\partial S_i/\partial t$). Relation between fixed and mobile concentrations for the species C_i is given by a combination of mass action and mass conservation equations. This leads to a highly nonlinear algebraic system which can be difficult to solve.[18] The well known Newton-Raphson method is often applied for the resolution of these equations.

When reactive transport systems are formulated in terms of kinetic reactions, this leads to a system of ordinary differential equations. The temporal derivative of chemistry is descretized using sub-time steps, which can be much smaller than the transport time step. There are many methods for solving this kind of equations and an extensive review can be found in Sandu et al.[19,20] In this work, we have chosen the well known fourth-order Runge-Kutta method since it is accurate, fast and simple to implement.

Results for Kinetic Reactions

In this section, SNIA_ELLAM and DSA_ELLAM are used to simulate advection dominated kinetic reactive transport problems. Performances of ELLAM with SNIA and DSA are assessed in comparing SNIA_ELLAM and DSA_ELLAM to SNIA_FE and DSA_FE for the cases of linear kinetic, nonlinear kinetic and interphase mass transfer problems.

First order decay problem

Efficiency of ELLAM with both SNIA and DSA is studied first for the simple case of transport with radioactive decay where the reaction term is proportional to the solute concentration. Boundary conditions are $C(0,t) = 1$, $C(\infty,t) = 0$ and the initial conditions $C(x,0) = 0$ for $x > 0$. The simulation time is $T = 400$ days. The domain is composed of a uniform grid, with $\Delta x = 20$ m and $l = 1000$ m. The parameters in Eq. 5 are $q = 1.0$ m/day, $R = 1$, $D = 0.01$ m^2/day, $K = 0.002$/day and $f = 0$. The exact analytical solution of this problem is known.[21]

Figure 2 shows results of DSA_FE using 50 time steps of 8 days (DSA_FE_ndt50) and 10 time steps of 40 days (DSA_FE_ndt10). Because standard FE is not suited for advection-dominated problems, a large numerical diffusion is obtained smearing the front for DSA_FE_ndt10. The numerical diffusion is reduced, but remains significant, with DSA_-FE_ndt50.

Results of DSA_ELLAM for this problem are obtained by solving the full system (6)–(7) on the moving mesh. Figure 2 shows the efficiency of ELLAM since the DSA_ELLAM results are in very good agreement with the analytical solution when using 50 time steps (DSA_ELLAM_ndt50). This is true with a single time step too (DSA_ELLAM_ndt1).

The first-order decay problem was studied to point out the mass balance error in the OS algorithm for problems involving continuous mass influx boundary conditions.[2] This error is inherent in the splitting of the reaction operator from the advection/dispersion operator; it exists even if each stage of the OS algorithm is solved exactly and tends to overestimate the amount of reaction.[2] Indeed, during the time step Δt, the exact solution states that mass is injected into the domain through the boundary at $x = 0$, and this mass undergoes simultaneous transport and decay. Therefore, mass input at the beginning of the time interval will undergo more decay than mass injected at the end of the time step. However, the OS formulation with standard Eulerian methods, states that all mass inputs during the time interval decay in the same way and over the same duration Δt; obviously, this will overestimate the amount of mass decayed.

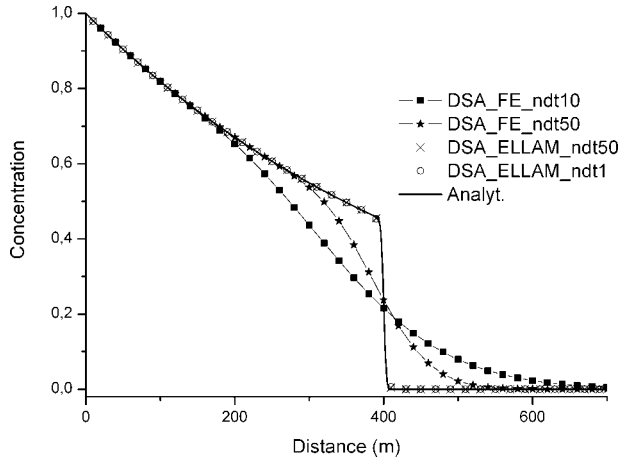

Figure 2. Results of DSA_FE and DSA_ELLAM for transport with first-order decay.

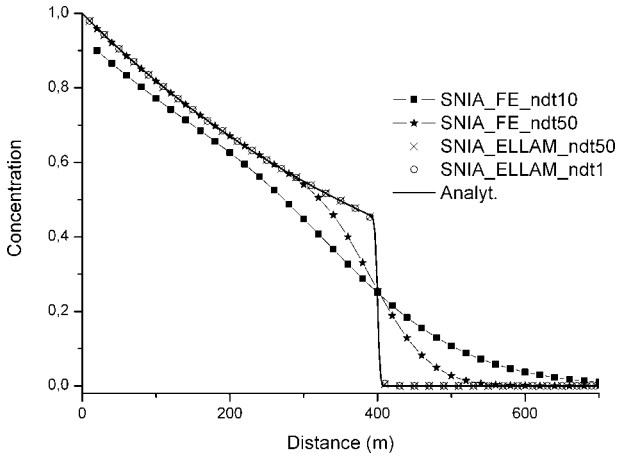

Figure 3. Results of SNIA_FE and SNIA_ELLAM for transport with first-order decay.

In Figure 3, both SNIA_FE_ndt10 and SNIA_FE_ndt50 results show significant numerical diffusion smearing the front (as with DSA_FE). Results of SNIA_FE_ndt10 show two kinds of errors. The first one is the numerical diffusion generated near the sharp front. The second one is the OS error due to continuous mass influx boundary condition. This error is proportional to the time step and becomes significant for large time steps.

To reduce the OS error, Valocchi and Malmstead[2] suggest a variant of the normal OS algorithm in which the order of solving advection-dispersion and reaction operators is reversed at each time step. In doing this, the alternating OS scheme overestimates during a first step but underestimates during the second step the proper amount of decayed mass. Hence, the mass errors for the first and second time steps are balanced, so that the overall error may be diminished.

The solution with SNIA_ELLAM is obtained in solving the advection dispersion equation (system (6)–(7) with $K = 0$) to obtain the transported concentration C_i^{transp} on the moving mesh, then followed by a reaction step using C_i^{transp} as initial concentration:

$$C_i^{n+1} = C_i^{\text{transp}} \exp(-K\Delta t_i) \tag{12}$$

Figure 3 shows the results from SNIA_ELLAM_ndt50 and SNIA_ELLAM_ndt1 with 50 time steps and a single one, respectively. Accurate results are obtained with SNIA_ ELLAM even with very large time steps. For this problem, the transport is solved accurately with ELLAM whatever the time step used and chemistry is solved analytically using Eq. 12. The OS mass balance errors described by Valocchi and Malmstead[2] and by Kaluarachchi and Morshed[3] are avoided since the time step for the dispersion integral in Eq. 7 and for chemistry in Eq. 12 is automatically adapted for elements near the inflow boundary.

The aerobic biodegradation transport problem

In this section, we simulate the nonlinear aerobic biodegradation transport problem given in Celia et al.[22] This is a three component system including substrate (aniline) concentration, electron acceptor (oxygen) concentration, and station-

ary biomass population. Many studies have shown the importance of microbial degradation of groundwater contaminants. In addition to natural biodegradation, one can encourage biodegradation of many organic contaminants by injecting appropriate nutrients to stimulate microbial activity.[22]

The set of transport equations is written as follows:

$$\begin{cases} \dfrac{\partial C_1}{\partial t}+\dfrac{\partial (q_1 C_1)}{\partial x}-\dfrac{\partial}{\partial x}\left(D_1\dfrac{\partial C_1}{\partial x}\right)+K_1(C_1,C_B)C_1=f_1(C_2,C_B) \\ \dfrac{\partial C_2}{\partial t}+\dfrac{\partial (q_2 C_2)}{\partial x}-\dfrac{\partial}{\partial x}\left(D_2\dfrac{\partial C_2}{\partial x}\right)+K_2(C_2,C_B)C_2=f_2(C_1,C_B) \end{cases} \tag{13}$$

The nonlinear reactions and source terms are given by

$$K_1(C_1,C_B)=\left(\frac{\mu_1 C_B}{K_h^1+C_1}\right)\delta_1, \qquad K_2(C_2,C_B)=\left(\frac{\mu_2 C_B}{K_h^2+C_2}\right)\delta_2$$

$$f_1(C_2,C_B)=-\kappa_{12}\left(\frac{\mu_2 C_B}{K_h^2+C_2}\right)C_2\delta_2$$

$$f_2(C_1,C_B)=-\kappa_{21}\left(\frac{\mu_1 C_B}{K_h^1+C_1}\right)C_1\delta_1 \tag{14}$$

C_α is the concentration of species α ($\alpha=1,2$), μ_α is the maximum uptake rate for species α, K_h^α is the half-saturation constant for species α, $\kappa_{\alpha\beta}$ denotes the yield ratio for species α when species β is limiting, δ_α equals one if species α is limiting and otherwise zero, C_B is the concentration of the stationary bacterial species considered constant.[16]

Linearization. The reaction coefficients and the right-hand side forcing functions are nonlinear. With DSA_ELLAM, a linearization technique can be applied to evaluate the coefficients in the governing equations using the previous (known) values of the solution. These can be values of the previous iteration or values of the previous time step. In both cases, the linearized equations are analogous to the linear variable Eq. 5.

To obtain $C_\alpha^{k+1}(x,t^{n+1})$ where k is the iteration index, we use the Gauss-Seidel-based approximations for both the first-order reaction coefficients and the right-hand side terms.[16]

$$K_1(C_1,C_B)=\left(\frac{\mu_1 C_B}{K_h^1+\overline{C_1^k}}\right)\delta_1, \quad K_2(C_2,C_B)=\left(\frac{\mu_2 C_B}{K_h^2+\overline{C_2^{k+1}}}\right)\delta_1$$

$$f_1(C_2,C_B)=-\kappa_{12}\left(\frac{\mu_2 C_B}{K_h^2+\overline{C_2^k}}\right)\overline{C_2^k}\delta_2$$

$$f_2(C_1,C_B)=-\kappa_{21}\left(\frac{\mu_1 C_B}{K_h^1+\overline{C_1^{k+1}}}\right)\overline{C_1^{k+1}}\delta_1 \tag{15}$$

with

$$\overline{C_\alpha^k}=\frac{1}{2}(C_\alpha^k(x,t^{n+1})+C_\alpha(x^*,t^n)) \tag{16}$$

Numerical Results. Parameter values are assigned as follows: $\mu_1=\mu_2=1.0$ day^{-1}, $K_h^1=K_h^2=0.1$ mg/l, $\kappa_{12}=2.0$, $\kappa_{21}=0.5, q_1=q_2=1$ m/day, $D=0.2$ m^2/day. Initial conditions are $C_1(x,0)=3.0$ mg/l, $C_2(x,0)=0$. Dirichlet conditions are specified at the inflow boundary $C_1(0,t)=3.0$ mg/l, $C_2(0,t)=10.0$ mg/l. Homogeneous Neumann conditions are specified at the outflow boundary. The fixed microbial concentration is $C_B(x,t)=0.2$ mg/l. The one-dimensional domain of size $l=100$ m is discretized with a constant space step of $\Delta x=1$ m and the simulation time is $T=60$ days.

With DSA_ELLAM, equations of the system are (13) solved in a sequential way using values of the solution from the previous iteration. The convergence is achieved when the following criteria are matched up:

$$\max_i|C_{1,i}^{k+1}-C_{1,i}^k|<\varepsilon \quad \text{and} \quad \max_i|C_{2,i}^{k+1}-C_{2,i}^k|<\varepsilon \tag{17}$$

For this example, we choose a tolerance $\varepsilon=10^{-5}$.

With SNIA_ELLAM, the linear advection dispersion equation is solved for both species to obtain transported concentrations. Then, these transported concentrations are used as initial concentrations for the following chemical system:

$$\begin{cases} \dfrac{\partial C_1}{\partial t}=-\kappa_{12}\left(\dfrac{\mu_2 C_B}{K_h^2+C_2}\right)C_2\delta_2-\left(\dfrac{\mu_1 C_B}{K_h^1+C_1}\right)C_1\delta_1 \\ \dfrac{\partial C_2}{\partial t}=-\kappa_{21}\left(\dfrac{\mu_1 C_B}{K_h^1+C_1}\right)C_1\delta_1-\left(\dfrac{\mu_2 C_B}{K_h^2+C_2}\right)C_2\delta_2 \end{cases} \tag{18}$$

This chemical system cannot be solved analytically as for the previous case. To obtain accurate solution, we use the fourth-order Runge-Kutta method with small time steps. Therefore, chemistry is solved with several small sub-time steps for one "large" time step of the transport operator. This procedure is not CPU time consuming since chemistry is solved locally (i.e. for each element without referring to the others).

With DSA_ELLAM, the number of time steps cannot be fixed. Indeed, when the iterative procedure does not converge for a given maximum number of iterations, the time step is reduced until the convergence is reached. The average number of time steps, the average time step size and the CPU time for various simulations with both SNIA_ELLAM and DSA_ELLAM are given in Table 1. Results of DSA_ELLAM_ndt300 are obtained using 300 time steps for the global implicit system. Those of SNIA_ELLAM_ndt1 are obtained using a single time step of 60 days for the transport followed by 200 sub-time steps for the chemistry operator. Good agreement is obtained between both simulations as shown in Figure 4.

Table 1 shows that, for the aerobic biodegradation transport problem, DSA_ELLAM is much more CPU time demanding than SNIA_ELLAM. Indeed, with DSA_ELLAM, many iterations are performed for each time step to reach the convergence. On the other hand, SNIA_ELLAM does not require convergence iterations.

Table 1. Comparison Between SNIA_ELLAM and DSA_ELLAM for the Biodegradation Problem

DSA_ELLAM			
Average number of time steps	30	120	300
Average time step size	2.0	0.5	0.2
$\overline{C}_2$	8.45	8.49	8.50
CPU (s)	0.08	0.13	0.69
SNIA_ELLAM			
Number of transport time steps	1	10	100
Number of chemistry sub-time steps	200	20	2
$\overline{C}_2$	8.5	8.5	8.5
CPU (s)	<0.01	<0.01	0.02

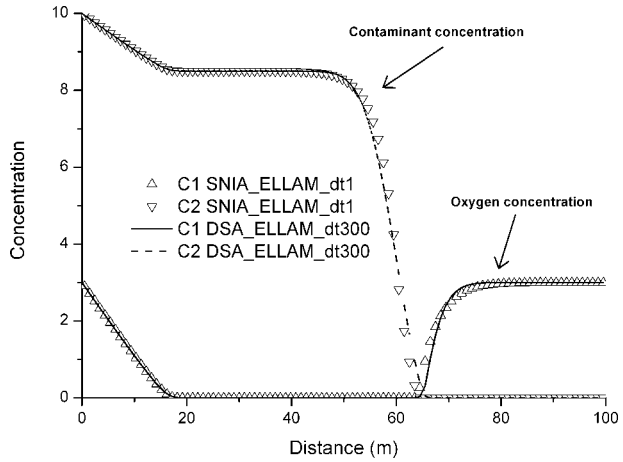

Figure 4. Results of DSA_ELLAM with 300 time steps and SNIA_ELLAM with a single transport time step for the aerobic biodegradation transport problem.

Since the concentration of the organic contaminant C_2 is the limiting factor behind the front area, the steady state value $\overline{C}_2$ behind the front should be 8.5 (see Celia et al.[22] for details). The values of $\overline{C}_2$ are given in Table 1 for all simulations. The DSA_ELLAM is much more sensitive to the number of time steps than SNIA_ELLAM. Indeed, the value of $\overline{C}_2$ improves with the increase of time steps in DSA_ELLAM. However, with SNIA_ELLAM, the value of $\overline{C}_2$ is independent of the time step size. This phenomenon is observed because the characteristic times of chemistry are smaller than that of transport. With SNIA_ELLAM, the chemistry is accurately solved with smaller sub-time steps than the time step of transport. This is not allowed with DSA_ELLAM since the same time step is used for both transport and chemistry operators.

Interphase mass transfer

In this section, SNIA_ELLAM and DSA_ELLAM are compared with SNIA_FE and DSA_FE for the simulation of heterogeneous kinetic reaction (in which the reactants are present in several phases). The problem involves advection, dispersion, and mass transfer processes. In general, mass transfer occurs between the fluid phase and two types of solid phase: (i) a fraction reaching rapidly equilibrium and (ii) a fraction reaching equilibrium slowly.[23] Transformation reactions are of general form and may be linear or non linear.[23] Interphase mass transfer with linear kinetic reaction was studied in Barry et al.[5] In this work, we consider the case of interphase mass transfer with nonlinear kinetic reaction. Subsets of this general model occur routinely in application, and because of this it makes a good test problem for the solution issues of concern in this work.

The governing one-dimensional solute transport equation with adsorption is given by:

$$\frac{\partial C}{\partial t}+\frac{\partial S}{\partial t}+\frac{\partial (qC)}{\partial x}-\frac{\partial}{\partial x}\left(D\frac{\partial C}{\partial x}\right)=0 \qquad (19)$$

Where C is the aqueous-phase solute concentration and S the solid-phase solute concentration. When the reaction is sufficiently fast, the concentration S is written as an algebraic function of C. Else, an additional differential equation must be used to solve Eq. 19. This results in the following kinetic law:

$$\frac{\partial S}{\partial t}=\alpha[f(C)-S] \qquad (20)$$

We consider the case of nonlinear sorption with $f(C)=kC^{nf}$. Parameters are assigned as follows: $q = 5 \times 10^{-4}$ m/day, $D = 5 \times 10^{-8}$ m^2/day, $\alpha = 0.001$, $k = 1$, and $nf = 0.7$. The one-dimensional domain of size $l = 1$ m is discretized with a uniform mesh of $\Delta x = 0.01$ m. The simulation time is $T = 1000$ days. Initial conditions are $C(x,0) = S(x,0) = 0$ mg/l. A Dirichlet condition is prescribed at the inflow boundary C $(0,t) = 1$ mg/l and an homogeneous Neumann condition defines the outflow boundary.

Many convergence problems have been encountered with FE simulations because of nonphysical oscillations. Indeed, it is well known that standard FE can lead to negative concentrations. These concentrations are not allowed due to the negative exponent in the Eq. 20. To obtain a monotonic scheme, we use an upwind finite element method and a mass lumping procedure to make the mass matrix diagonal.

In Figure 5, results of DSA_FE and DSA_ELLAM with 20 and 200 time steps are compared to a reference solution calculated with standard FE with a very fine space and time discretization. As for the first-order decay problem, results from DSA_FE_ndt20 show important numerical diffusion for both C and S. The numerical diffusion is reduced for smaller time steps (DSA_FE_ndt200). Because of numerical diffusion, no convergence problems are encountered with DSA_FE when using large time steps (even with 10 time steps).

Highly accurate results are obtained with DSA_ELLAM_ndt200 as shown in Figure 5. Decreasing the number of time steps reduces accuracy (see, e.g. DSA_ELLAM_ndt20, in Figure 5) and in addition, when large time steps are used, convergence problems may be encountered. For example DSA_ELLAM does not reach the convergence when used with only 10 time steps.

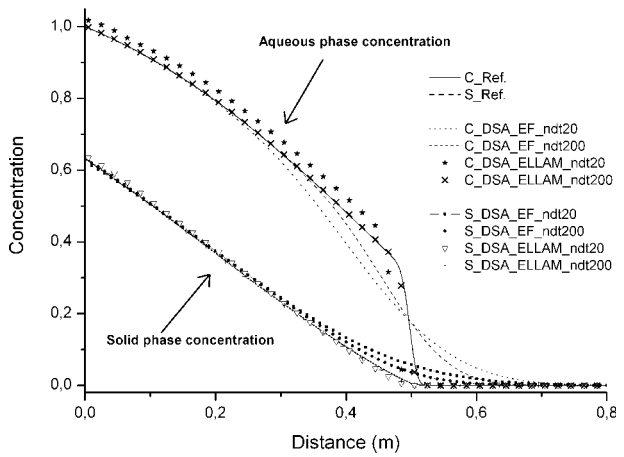

Figure 5. Results of DSA_FE and DSA_ELLAM for the interphase mass transfer problem.

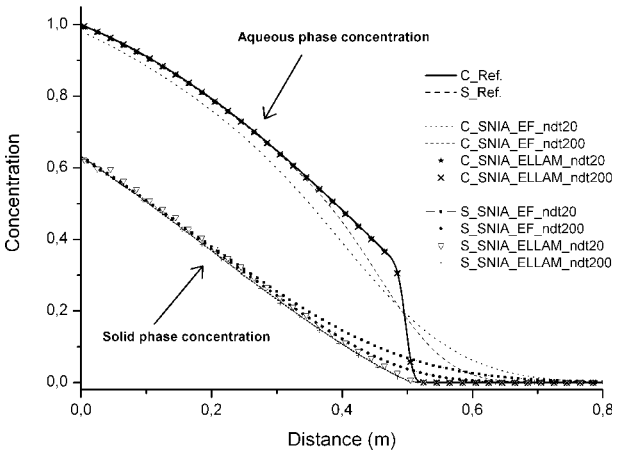

Figure 6. Results of SNIA_FE and SNIA_ELLAM for the interphase mass transfer problem.

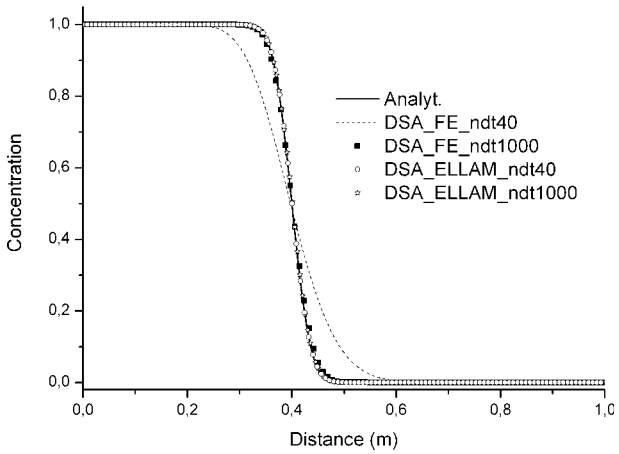

Figure 7. Results of DSA_FE and DSA_ELLAM for the linear adsorption problem.

Results of SNIA_ELLAM and SNIA_FE with 20 and 200 time steps are plotted in Figure 6. As for the first-order decay problem, SNIA_FE with small time steps (SNIA_FE_ndt200) leads to a solution with numerical diffusion smearing the front. The results from SNIA_FE_ndt20 show numerical diffusion and an OS error due to continuous mass injection at the inlet boundary condition. Both errors are cancelled with SNIA_ELLAM. High accurate results are obtained with SNIA_ELLAM_ndt20 since the chemistry operator is solved with sub-time steps smaller than the transport time step. The number of chemistry sub-time steps is 10 for SNIA_ELLAM_ndt20 and 1 for SNIA_ELLAM_ndt200.

To sum up, the numerical experiments dealing with a first-order decay, a Monod biodegradation and an interphase mass transfer have shown SNIA_ELLAM to be highly accurate and efficient because:

- The moving mesh ELLAM gives accurate results for the transport operator even for advection dominated problems with large time steps;
- Chemistry can be solved accurately with specific methods and smaller time steps than that used for the transport operator;
- The mass balance error present in the OS algorithm for problems with continuous mass injection at the inlet boundaries is avoided.

Results for Equilibrium Reactions

In this section, SNIA_ELLAM and DSA_ELLAM are used to simulate advection-dominated transport coupled with sorption reactions at equilibrium. Performances of ELLAM with SNIA and DSA are assessed in comparing SNIA_ELLAM and DSA_ELLAM with SNIA_FE and DSA_FE for both linear and nonlinear equilibrium.

The linear adsorption problem

The following linear adsorption problem is considered:

$$\frac{\partial C}{\partial t}+\frac{\partial S}{\partial t}=D\frac{\partial^2 C}{\partial x^2}-V\frac{\partial C}{\partial x}, \qquad S=K_{\mathrm{R}}C \tag{21}$$

With $K_R = 4$, $V = 1$ m/day, $D = 10^{-3}$ m^2/day. The domain of size $l = 1$ m is discretized at the constant space step $\Delta x = 10^{-3}$ m and the simulation time is $T = 2$ days.

Results of DSA_FE and DSA_ELLAM with 40 and 1000 equal time steps are plot in Figure 7. DSA_FE with large time steps (DSA_FE_ndt40) yields non-negligible numerical diffusion smearing the sharp front and accurate results require computations with small time steps (DSA_FE_ndt1000). On the other hand, DSA_ELLAM gives accurate results with both small and large time steps (DSA_ELLAM_ndt40 and DSA_ELLAM_ndt1000).

The linear sorption problem is also simulated with SNIA_FE and SNIA_ELLAM using 40 and 1000 time steps but the results are less accurate. As stated by Herzer and Kinzelbach[24] and Barry et al.[6] SNIA_FE and SNIA_ELLAM (Figure 8) show that OS errors generate a numerical diffusion proportional to Δt which becomes therefore significant for large time steps (e.g., SNIA_FE_nd40 and SNIA_ELLAM_ndt40 in Figure 8). The ELLAM approach remains, however, less subject to numerical diffusion than the FE.

The nonlinear sorption problem

In this problem sorption reactions are modeled with a local equilibrium assumptions and the nonlinear Freundlich equilib-

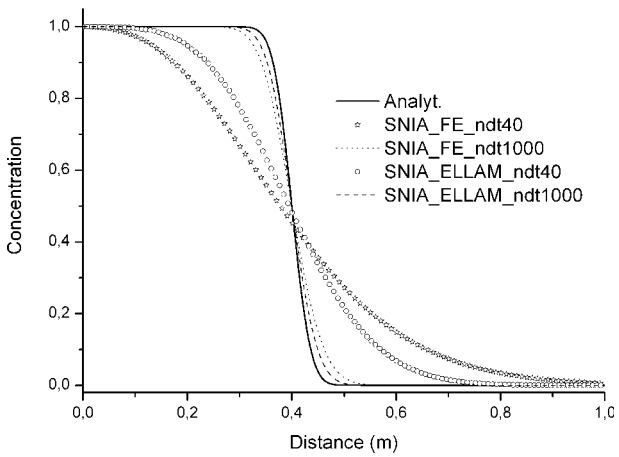

Figure 8. Results of SNIA_FE and SNIA_ELLAM for the linear adsorption problem.

rium isotherm. This model is relevant because it may be used as at least a first-cut approximation for the transport of a large number of neutral hydrophobic solutes through porous media that include soils, sediments, and aquifer materials.[15]

The problem was studied by Farthing et al.[15] and corresponds to the transport with the so called problem of "self-sharpening" front. The test problem is a constant injection into a domain initially free of contaminant. Transport is governed by advection and dispersion of the solute in the aqueous phase coupled with sorption onto the solid phase following an instantaneous local equilibrium with a Freundlich isotherm:

$$\frac{\partial C}{\partial t}+\frac{\rho_b}{\theta}\frac{\partial (K_f C^{nf})}{\partial t}+U\frac{\partial C}{\partial x}=\frac{\partial}{\partial x}\left(D\frac{\partial C}{\partial x}\right) \tag{22}$$

where $\rho_b = 1.59$ is the bulk density of the solid phase, $\theta = 0.4$ the porosity, $K_f = 2.26$ the sorption capacity coefficient and $nf = 0.7$ the exponent measuring the sorption intensity. Transport parameter values are assigned as follows: $U = 1.0$ m/day and $D = 10^{-3}$ m^2/day. Initial condition is $C(x,0) = 0$. A Dirichlet condition is prescribed at the inflow boundary $C(0,t) = 1.0$ mg/L as well as a null diffusive flux at the outflow boundary. The domain consists of a uniform grid, with $\Delta x = 0.02$ m over $l = 10$ m and the simulation time is $T = 60$ days.

In this case, the characteristic velocity $(\lambda = U/R_f)$ depends on the unknown concentration and the retardation factor R_f is given by,

$$R_f = 1 + nf\frac{\rho_b}{\theta}K_f C^{nf-1} \tag{23}$$

The equivalent retardation coefficient in the original Farthing et al.[15] problem is about 1.5. In our case, the sorption capacity coefficient is increased in order to have an important retardation factor of about 10. Results of SNIA_ELLAM and DSA_ELLAM with both 200 and 1000 time steps are plotted in Figure 9. Table 2 gives the CPU time for each simulation.

SNIA_ELLAM gives results with numerical diffusion proportional to the time step and requires small time steps to provide an accurate solution, as observed for the case of the linear adsorption problem. DSA_ELLAM is more efficient than SNIA_ELLAM. Indeed, DSA_ELLAM with only 10 time steps requires 0.1 s of CPU time and gives more accurate solution than SNIA_ELLAM with 1000 time steps, which requires 0.7 s of CPU time. Figure 9 also shows that DSA_ELLAM is not very sensitive to the time step size since results computed with 200 time steps do not significantly improve when compared with those obtained in 10 time steps.

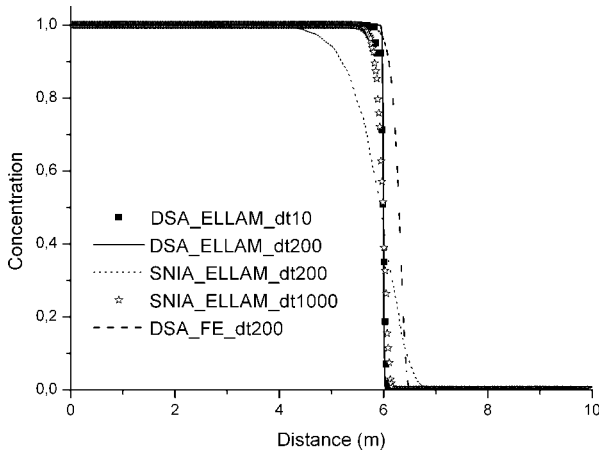

Figure 9. Results of the nonlinear sorption problem with SNIA_ELLAM, DSA_ELLAM, and DSA_FE.

Table 2. Comparison Between SNIA_ELLAM and DSA_ELLAM for the Nonlinear Sorption Problem

	SNIA_ELLAM		DSA_ELLAM		DSA_FE
Nb time steps	200	1000	10	200	200
CPU (s)	0.17	0.7	0.1	1.0	0.7

To avoid nonphysical oscillations with FE, a mass lumping procedure combined with an upwind scheme is applied. Even for this self-sharpening front problem, the method is hampered with important numerical diffusion. Results of DSA_FE_ndt200 are less accurate than those of DSA_ELLAM_ndt10 (Figure 9). Further, we notice that results of SNIA_ELLAM_ndt1000 requires the same CPU time than DSA_FE_ndt200. However, results of SNIA_ELLAM_ndt1000 are much more accurate than those of DSA_FE_ndt200 (Figure 9).

To conclude, the numerical experiments for both linear and nonlinear equilibrium reactions show that:

- Contrarily to kinetic reactions, OS errors with equilibrium reactions induce numerical diffusion which cannot be removed with SNIA_ELLAM;
- SNIA_ELLAM requires small time steps to give the accurate solution;
- DSA_ELLAM is not very sensitive to the time step size and is much more accurate than SNIA_ELLAM;
- DSA_ELLAM is more accurate and more efficient than DSA_FE.

Conclusion

The moving mesh ELLAM was combined with DSA and SNIA to accurately solve advection-dominated reactive transport problems. SNIA_ELLAM and DSA_ELLAM were compared to SNIA_FE and DSA_FE for (1) kinetic reactions with first-order decay, Monod biodegradation, and interphase mass transfer problems and (2) equilibrium reactions with linear and nonlinear sorption problems.

Results for all the kinetics problems (first-order decay, Monod biodegradation, interphase mass transfer) show that SNIA_ELLAM can be highly accurate and efficient since the transport operator is solved with the moving mesh ELLAM which gives accurate results for advection-dominated problems even with large time steps. The chemistry operator is solved accurately with specific methods and smaller time steps than for transport. Moreover, the mass balance errors present in the OS algorithm for problems involving continuous mass injection at inlet boundaries are avoided.

For equilibrium reactions, SNIA_ELLAM induces numerical diffusion proportional to the time step size. SNIA_ELLAM remains more accurate (with less numerical diffusion) than SNIA_FE. Results from the DSA_FE show numerical diffusion whereas DSA_ELLAM avoids artificial diffusion and is the more efficient and accurate method in this case.

Literature Cited

1. Saaltink MW, Careera J, Ayora C. On the behaviour of approaches to simulate reactive transport. *J Contam Hydrol*. 2001;48:213–235.
2. Valocchi AJ, Malmstead M. Accuracy of operator splitting for advection-dispersion reaction problems. *Water Resour Res*. 1992; 28:1471–1476.
3. Kaluarachchi JJ, Morshed J. Critical assessment of the operator-splitting technique in solving the advection-dispersion-reaction equation: 1. First-order reaction. *Adv Water Resour*. 1995;18:89–100.
4. Morshed J, Kaluarachchi JJ. Critical assessment of the operator-splitting technique in solving the advection-dispersion-reaction equation. II. Monod kinetics and coupled transport. *Adv Water Resour*. 1995; 18:101–110.
5. Barry DA, Bajracharya K, Miller CT. Alternative split-operator approach for solving chemical reaction/groundwater transports models. *Adv Water Resour*. 1996;19:261–275.
6. Barry DA, Miller CT, Culligan PJ, Bajracharya K. Analysis of split operator methods for nonlinear and multispecies groundwater chemical transport models. *Maths Comput Sim*. 1997;43:331–341.
7. Yeh GT, Tripathi VS. A critical evaluation of recent developments in hydrogeochemical transport models of reactive multichemical components. *Water Resour Res*. 1989;25:93–108.
8. Miller CT, Rabideau AJ. Development of split-operator, Petrov-Galerkin methods to simulate transport and diffusion problems. *Water Resour Res*. 1993;29:2227–2240.
9. Carrayrou J, Mosé R, Behra P. New efficient algorithm for solving thermodynamic chemistry. *AIChe J*. 2002;48:894–904.
10. Younes A. An accurate moving grid Eulerian Lagrangian localized adjoint method for solving the one-dimensional variable-coefficient ADE. *Int J Numer Meth Fluids*. 2004;45:157–178.
11. Celia MA, Russell TF, Herrera I, Ewing RE. An Eulerian-Lagrangian localized adjoint method for the advection-diffusion equation. *Adv Water Resour*. 1990;13:187–206.
12. Russell TF, Celia MA. An overview of research on Eulerian-Lagrangian localized adjoint methods (ELLAM). *Adv Water Resour*. 2002; 25:1215–1231.
13. Bell LSJ, Binning PJ. A split operator approach to reactive transport with the forward particle tracking Eulerian Lagrangian localized adjoint method. *Adv Water Resour*. 2004;27:323–334.
14. Wang H, Ewing RE, Celia MA. Eulerian-Lagrangian localized adjoint method for reactive transport with biodegradation. *Numer Meth Part Differ Equat*. 1995;11:229–254.
15. Farthing MW, Kees CE, Russell TF, Miller CT. An ELLAM approximation for advective-dispersive transport with nonlinear sorption. *Adv Water Resour*. 2006;29:657–675.
16. Vag JE, Wang H, Dahle HK. Eulerian-Lagrangian localized adjoint methods for systems of nonlinear advective-diffusive-reactive transport equations. *Adv Water Resour*. 1996;19:297–315.
17. Ruan F, Mclaughlin D. An investigation of Eulerian-Lagrangian for solving heterogeneous advection-dominated transport problems. *Water Resour Res*. 1999;35:2359–2373.
18. Walsh MP, Bryant SL, Schechter RS, Lake LW. Precipitation and dissolution of solids attending flow through porous media. *AIChe J*. 1984;30:317–328.
19. Sandu A, Verwer JG, van Loon M, Carmichael GR, Potra FA, Dabdub D, Seinfeld JH. Benchmarking stiff ODE solvers for atmospheric chemistry problems 1. Implicit vs explicit. *Atmos Environ*. 1997;31:3151–3166.
20. Sandu A, Verwer JG, Blom JG, Spee EJ, Carmichael GR, Potra FA. Benchmarking stiff ODE solvers for atmospheric chemistry problems 2. Rosenbrock solvers. *Atmos Environ*. 1997;31:3459–3472.
21. Ogata A, Banks RB. A solution of the differential equation of longitudinal dispersion in porous media. *Geol Surv Prof Pap US*. 1961; 411-A.
22. Celia MA, Kindered JS, Herrera I. Contaminant transport and biodegradation. I. A numerical model for reactive transport in porous media. *Water Resour Res*. 1989;25:1141–1148.
23. Kanney JF, Miller CT, Barry DA. Comparison of fully coupled approaches for approximating nonlinear transport and reaction problems. *Adv Water Resour*. 2003;26:353–372.
24. Herzer J, Kinzelbach W. Coupling of transport and chemical processes in numerical transport models. *Geoderma*. 1989;44:115–127.

Manuscript received Dec. 7, 2006, and revision received May 20, 2007.